Budownictwo i Architektura 22(4) 2023, 71-95

DOI: 10.35784/bud-arch.5491
Received: 22.10.2023; Revised: 26.11.2023;
Accepted: 20.12.2023; Available online: 29.01.2024

Orginal Article

Engineering properties of self-compacting concrete incorporating PET fibres and recycled fine concrete aggregates

Meriem Bayah[1,2], Farid Debieb[2], El-Hadj Kadri[3], Mohamed Bentchikou[4]

[1] Civil Engineering Department, Faculty of Technology, University Saad Dahleb of Blida, Algeria; P.O. Box 270, 09000 Blida, Algeria;
meriembayah@gmail.com
[2] Materials and Environment Laboratory, University Yahia Fares of Medea, Algeria; P.O. Box 164, Urban Pole, 26000 Médéa, Algeria;
f_debieb@yahoo.com; ORCID 0000-0002-3898-7037
[3] L2MGC - Civil Engineering Mechanics and Materials Laboratory, University of Cergy-Pontoise, France; 33 Bd du Port, 95000 Cergy, France;
el-hadj.kadri@u-cergy.fr; ORCID 0000-0001-7383-8574
[4] Mechanic-Physic and Mathematic Modelling Laboratory, University Yahia Fares of Medea, Algeria; P.O. Box 164, Urban Pole, 26000 Médéa, Algeria;
bentchikou_moham@yahoo.com

Abstract: Concrete is currently the most frequently used material in the building sector due to its favourable properties. However, the proliferation of waste poses a significant environmental problem. Over the past three decades, researchers have explored the use of construction and demolition waste (CDW) as well as plastic waste as aggregates, binders, and fibres in construction materials. This approach has emerged as a notable solution to address environmental and economic challenges. The objective of this research is to assess the impact of polyethylene terephthalate fibres (PETF) on the behaviour of self-compacting concrete (SCC) with recycled fine concrete aggregates (RFCA). Natural fine aggregates (NFA) were used as a substitute for RFCA at different mass fractions (0–100%). Additionally, four volumetric fractions (V_f) of PETF (ranging from 0.3% to 1.2%) were added, and the findings revealed an improvement in the flexural strength and modulus of elasticity of the composite material obtained. However, as the V_f content of PET fibres and RFCA increased, the compressive strength decreased, negatively affecting water absorption by immersion and capillary water absorption. Using 100% RFCA and 1.2% PETF enhanced the modulus of elasticity and flexural strength of recycled self-compacting concrete (RSCC) by up to 25% and 9%, respectively.

Keywords: polyethylene terephthalate fibres, recycled fine concrete aggregates, flexural strength, self-compacting concrete

1. Introduction

Currently, the world is witnessing an increase in construction and demolition waste (CDW), with approximately 60% of this waste being disposed of in landfill, leading to serious environmental problems [1,2]. On the other hand, there is a growing demand for natural resources driven by rapid development in the construction industry. Thus, it is possible to recycle waste concrete and use it as a substitute for these resources in the form of recycled concrete aggregates (RCA). The utilisation of RCA is considered a practical and sustainable solution to conserve natural resources and alleviate environmental strain [3],[4]. However, the surface structure of these RCA particles differs significantly from natural aggregates (NA) particles, primarily because of the presence of attached mortar. The recycled aggregate concrete (RAC) exhibits an inferior performance compared to the concrete made with NA [5,6], such as workability [7],[8], mechanical properties [5 ,9], and durability [10] ,[11]. The negative results of RAC are dependent on the high coefficient of water absorption, the porosity of the mortar adhering to them, and the less robust interface transition zones (ITZs) between attached mortar and NA. Therefore, researchers are working to improve the behaviour of RAC using different methods, such as controlling the water-cement ratio, employing chemical and mineral admixtures correctly, and applying the right preparation techniques before using RCA, as well as steel fibre (SF), polypropylene (PP) fibre, and glass fibre (GF) [12]–[14]. Several studies have shown that nearly all types of fibres can improve the mechanical qualities of concrete, such as ductility, tensile strength, and flexural strength [15], [16].

The use of fibre reinforcement in recycled aggregate concrete has attracted the attention of scholars. In recent years, numerous studies have explored its mechanical properties. Al-Hadithi et al. [16] examined the properties of fresh and mechanical aspects of self-compacting concrete (SCC) containing varying amounts of recycled PETF and determined that SCC containing 1.5% PETF exhibited the highest compressive and flexural strength. Bui et al. [17] carried out an investigation into recycled PETF and recycled woven bag fibre-reinforced recycled aggregate concrete (RAC), and the findings indicated that the incorporation of recycled plastic fibres not only enhanced flexural and tensile strength but also reduced drying shrinkage and shrinkage cracking in RAC. App Hajmohammadian et al. [18] investigated the workability and mechanical characteristics of RAC reinforced with PP fibres, and the findings showed that introducing PP fibres reduced the workability of the concrete while simultaneously increasing both compressive and tensile strength. Dong et al. [19] conducted a study on recycled plastic fibre-reinforced recycled self-compacting concrete (RSCC) to examine its fresh and hardened properties. Toghroli et al. [20] studied the effect of recycled concrete aggregate (RCA) and pozzolanic materials on the mechanical and permeability properties of fibre-reinforced concrete. They cast a total of 110 concrete mixes, with RCA being used to partially replace natural coarse aggregate (NCA) at various levels (25%, 50%, 75%, and 100%) by weight. Steel fibre (ST) and waste plastic fibre (WPF) were introduced at 1% and 2% volume fractions. Their findings demonstrated a 25% increase in permeability and a 60% loss in the strength qualities of mixes containing 100% RCA. However, the inclusion of fibres resulted in increases in compressive and flexural strength.

Numerous studies have explored concrete incorporating RCA particles, but there is limited research on the impact of combining RCA particles with recycled PET fibres on concrete performance. Consequently, in this experimental programme, our objective was to create and improve the performance of concrete by incorporating (25%, 50%, 75%, and 100%) RFCA particles and varying volume percentages (ranging from 0.3% to 1.2%) of

recycled PET fibres. At 90 days of age, this programme includes compressive strength, flexural strength, modulus of elasticity, and water absorption.

2.Methods and Materials

2.1. Materials and mix design

The components employed in this experiment consisted of cement, water, natural coarse, RFCA, PET fibre, fine aggregates, and a superplasticiser. Fine aggregate with a maximum size of 4 mm was obtained from natural dune sand. Two sizes of natural coarse aggregates (NCA), 3/8 and 8/15, were used. RFCA were produced by crushing laboratory-made concrete slabs with a compressive strength of 25 MPa (age 28 days of water curing). Initially, manual crushing was employed before final processing using mechanical crushers to achieve smaller pieces. Subsequently, the crushed material underwent sieving to attain RFCA with a targeted size, approximately 4 mm (see Fig.1). Tables 1-2 provide details on the physical and chemical properties of NCA, NFA, and RFCA, respectively. The chemical compositions were determined using the X-ray fluorescence (XRF) test. Additionally, the particle size distribution of NCA, NFA, and RFCA is illustrated in Fig. 2.

In this study, Portland cement type two (CEM II/B) with a compressive strength of 42.5 MPa was used. The cement had a specific surface area of 3900 cm^2/g, a density of 3.08 kg/m^3, and its chemical properties are detailed in Table 2. A polycarboxylate superplasticiser (SP) was employed at dosages ranging from 0.5% to 2% by the mass of powder. This superplasticiser had a specific gravity of 1.07 and a pH level of 6. PET fibre, measuring 30 mm in length and 0.44 mm in diameter, was produced by recycling waste plastic bottles. After the collection of waste bottles, they underwent a grinding process to obtain shredded material. Subsequently, the material underwent extrusion to produce filaments with the specified diameter, necessitating a subsequent cutting step to achieve fibres with a length of 30 mm. The texture and morphology of the fibre can be observed in Fig. 3. It possesses a typical tensile strength of 383 MPa, Young's modulus of 7.17 GPa, and an elongation to break of 53%.

Table 3 provides a summary of twenty-five mix proportions of Self-Compacting Concrete (SCC) with varying replacement rates of RFCA and different fibre content levels. The NFA was partially replaced by RFCA at the levels of 0%, 25%, 50%, 75%, and 100% by weight. The SCC mixes were designed in five families, denoted as A, B, C, D, and E. Each family comprised five concrete mixes, with PET fibre added by volume at 0.3%, 0.5%, 1%, and 1.2%. The code "25 RFCA-0.5 PETF" indicates self-compacting concrete mixes prepared with 25% RFCA as NFA replacement and 0.5% PETF as an additive.

In this study, the creation of SCC mixes involved three mixing steps. Initially, cement, aggregates, and fibres were briefly mixed for 30 seconds. After the addition of 70% of the mixing water, the mixture was stirred for 1 minute. Subsequently, the remaining 30% of water, which contained the superplasticiser, was added and mixed for an additional minute. This procedure continued for another 5 minutes before a 2-minute pause. To ensure the consistency of the mixes, the SCC was mixed once more for 30 seconds before discharge.

Table 1. The chemical composition of cement and fine aggregates. *Source:* own study

Composition (%)	Cement	NFA	RFCA
SiO_2	15.96	92.86	9.58
CaO	62.17	0.37	49.40
CO_2	11.46	0.64	38.76
Fe_2O_3	2.75	0.25	0.91
Al_2O_3	3.75	2.52	2.43
MgO	1.33	0.13	1.54
Na_2O	0.12	0.04	-
K_2O	0.52	1.01	0.20
SO_3	2.30	0.30	2.75

Table 2. The physical characteristics of aggregates. *Source:* own study

Type of aggregates	NCA	NCA	NFA	RFCA
Maximum Size (mm)	15	8	4	4
Bulk density (g/ cm^3)	1.52	1.50	1.59	1.24
Specific density (g/cm^3)	2.61	2.63	2.65	2.40
Fineness Modulus	-	-	2.24	3.01
Los Angeles Abrasion (%)	26.5	27.5	-	-
Water absorption (%)	0.59	0.79	0.65	8.5

Fig. 1. Production process of RFCA. *Source*: own study

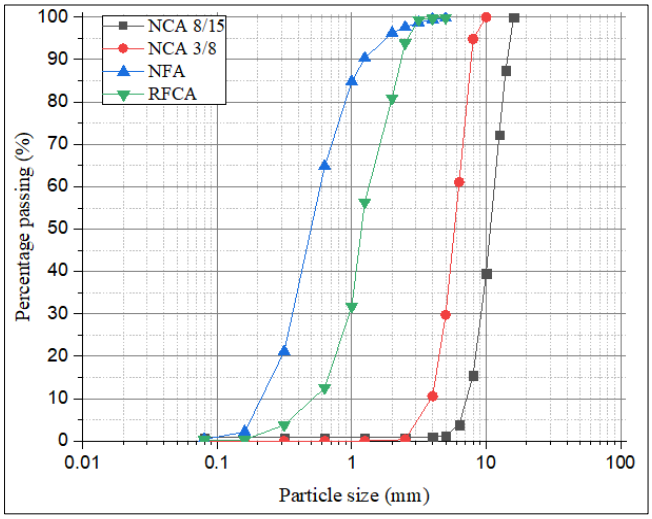

Fig. 2. The particle size distribution curves of both natural and recycled aggregates. *Source*: own study

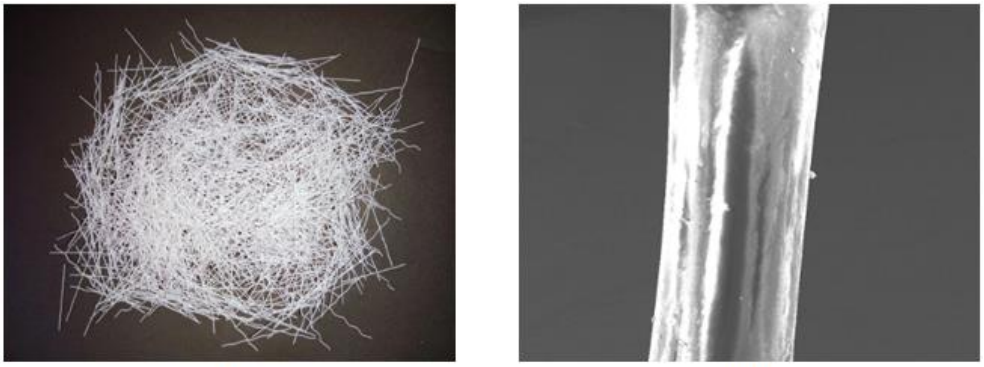

Fig. 3. PET fibres: (a) texture; (b) morphology. *Source*: own study

Table 3. Mix proportion. *Source*: own study

Specimens		NFA (kg)	NCA (kg)	RFCA (kg)	Cement (kg)	SP (kg)	PETF (%)	W/B
	Control mix	922.43	750.04	-	483.69	4.60	-	0.4
A	0RFCA-0.3PETF	922.43	750.04	-	483.69	4.69	0.3	0.4
	0RFCA-0.5PETF	922.43	750.04	-	483.69	4.69	0.5	0.4
	0RFCA-1PETF	922.43	750.04	-	483.69	4.84	1	0.4
	0RFCA-1.2PETF	922.43	750.04	-	483.69	4.84	1.2	0.4
B	25RFCA-0PETF	691.82	750.04	230.60	483.69	4.60	-	0.4
	25RFCA-0.3PETF	691.82	750.04	230.60	483.69	4.69	0.3	0.4
	25RFCA-0.5PETF	691.82	750.04	230.60	483.69	4.69	0.5	0.4
	25RFCA-1PETF	691.82	750.04	230.60	483.69	4.84	1	0.4
	25RFCA-1.2PETF	691.82	750.04	230.60	483.69	4.84	1.2	0.4

Specimens		NFA (kg)	NCA (kg)	RFCA (kg)	Cement (kg)	SP (kg)	PETF (%)	W/B
C	50RFCA-0PETF	461.21	750.04	461.21	483.69	4.60	-	0.4
	50RFCA-0.3PETF	461.21	750.04	461.21	483.69	4.69	0.3	0.4
	50RFCA-0.5PETF	461.21	750.04	461.21	483.69	4.69	0.5	0.4
	50RFCA-1PETF	461.21	750.04	461.21	483.69	4.84	1	0.4
	50RFCA-1.2PETF	461.21	750.04	461.21	483.69	4.84	1.2	0.4
D	75RFCA-0PETF	230.60	750.04	691.82	483.69	4.60	-	0.4
	75RFCA-0.3PETF	230.60	750.04	691.82	483.69	4.69	0.3	0.4
	75RFCA-0.5PETF	230.60	750.04	691.82	483.69	4.69	0.5	0.4
	75RFCA-1PETF	230.60	750.04	691.82	483.69	4.84	1	0.4
	75RFCA-1.2PETF	230.60	750.04	691.82	483.69	4.84	1.2	0.4
E	100RFCA-0PETF	-	750.04	922.43	483.69	4.60	-	0.4
	100RFCA-0.3PETF	-	750.04	922.43	483.69	4.69	0.3	0.4
	100RFCA-0.5PETF	-	750.04	922.43	483.69	4.69	0.5	0.4
	100RFCA-1PETF	-	750.04	922.43	483.69	4.84	1	0.4
	100RFCA-1.2PETF	-	750.04	922.43	483.69	4.84	1.2	0.4

2.2. Test procedures

2.2.1. Fresh concrete tests

The fresh tests were carried out following the guidelines outlined in the EFNARC-2005 [21] Standards for SCC. V-funnel, Slump flow, segregation resistance, and L-box tests were performed on every fresh mixture to evaluate viscosity, filling capacity, resistance to segregation, and flowability.

According to the European standard (EN 12350-8) [22], the slump flow test was used to evaluate the flowability and flow rate of SCC. Fresh concrete is poured into a cone positioned on a steel plate for this test. After the concrete has stopped flowing, the diameter of the concrete spread in the longitudinally perpendicular direction is measured. The diameter of the slump flow is normally between 550 and 850 mm.

The V-funnel test was performed in accordance with EN 12350-9 [22] to measure the filling capacity of SCC. The flow time of SCC can be measured using a V-shaped funnel in this test. The measured time is the amount of time it takes for fresh concrete to flow out of the V-funnel.

The L-box and sieve stability tests were performed to assess the passing ability and stability of SCC. In the L-box test, fresh concrete is placed into the vertical section of the L-box, and after 1 minute of rest, the gate is raised to allow the concrete to flow into the horizontal section of the box between the reinforcing bars without segregation or blockage. The ratio H2/H1 is then determined in accordance with the European standard EN 12350-10 [23], where H1 represents the depth of concrete immediately behind the gate and H2 corresponds to the end of the box's horizontal portion. According to EN 12350-11 [24], the sieve stability values must be in the range of 0-15%.

2.2.2. Hardened concrete tests

In this research, we examined the cube compressive strength, flexural strength, and elastic modulus of hardened concrete specimens. Three 100 × 100 × 100 mm cubes were

constructed for each specimen and cured for 90 days in line with BSI 12390-3 [25]. Additionally, three 100 × 200 mm cylindrical specimens were constructed in accordance with ASTM C469-02 [26] criteria to evaluate the elastic modulus.

According to the Standard test technique for flexural strength described in EN 12390-5 [27], the flexural strength test was conducted using the three-point loading method with three prismatic samples measuring 70 × 70 × 280 mm at the age of 90 days.

The water absorption by immersion tests were conducted on cubic specimens following the guidelines of BS 1881-122 [28]. These specimens were initially cured in water at 22°C for a duration of 90 days. Subsequently, the specimens were subjected to a drying process in an oven at 60°C for a minimum of 10 days. In cases where the discrepancy between the results obtained from two consecutive mass measurements exceeded 0.5% of the smaller value, the specimens were reweighed to obtain the value M_1. After the curing period, the specimens were submerged in a water tank for 7 days, and then they were weighed using a balance with a precision of 0.01 grams, after being wiped with a dry paper towel. Subsequently, they were weighed again to obtain the value M_2. The absorption rate is calculated as follows:

$$Ab(\%) = \frac{M_2 - M_1}{M_1} \cdot 100 \tag{1}$$

where: Ab: the absorption rate in %; M_1: the mass of the specimen in a saturated state in kg; M_2: the mass of the specimen in a dry state in kg.

The capillary absorption test involves measuring the mass of water absorbed by pre-conditioned concrete specimens following the recommendations of the ASTM [29] procedure. The test was conducted at the age of 90 days on moulded samples in the shape of 100 mm cubic specimens. These specimens were dried in a ventilated and controlled oven until a constant mass was achieved ($\Delta M < 0.1\%$ in 24 hours). The lateral faces of the specimens were covered with a thin layer of resin to ensure unidirectional flow and prevent lateral evaporation of absorbed water. The capillary absorption test is performed following this pre-conditioning. Capillary absorption is calculated at any given time as the ratio of the sample's mass increase to the area of contact with water.

3. Test results and discussions

3.1. Fresh concrete properties

3.1.1. Slump flow

All the mixtures met the EFNARC requirement [21] for deformability, as indicated by a slump flow diameter falling within the range of 767.5 mm to 650 mm, as shown in Fig. 4. This suggests that PET fibre-reinforced RFCA-SCC displayed limited filling ability. Furthermore, as shown in Fig. 4, there is a slight decrease in slump flow value as RFCA content increases, implying that the addition of RFCA has a negative influence on the workability of SCC. The slump flow values for mixtures containing 25%, 50%, 75%, and 100% RFCA-SCC (without PET fibre) decreased by 1.31%, 4.57%, 8.15%, and 10.1%, respectively, compared to the reference SCC. This reduction can be attributed to the higher water absorption capacity of RFCA in comparison to NFA, aligning with the findings of Carro-Lopez [30]. The diameter reduction may have been aggravated by the presence of a large amount of fine particles in the granulometric composition of RFCA, which showed a larger specific area, providing a larger adsorption surface [31].

Fig. 4 depicts the effect of PET fibre on the slump flow diameter of RFCA-SCC mixes, where the slump flow value is shown against the PET fibre replacement ratio under various RFCA replacement ratios. For example, when compared to the companion control 100RFCA-SCC, the slump flow values of 100RFCA-0.3PETF, 100RFCA-0.5PETF, 100RFCA-1PETF, and 100RFCA-1.2PETF reduced by 1.45%, 2.89%, 3.76%, and 5.79%, respectively. Al Hadithi et al. [32] discovered that the slump flow diameter reduced as the PET fibre concentration increased. This reduction can be attributed to the fibres' tendency to cluster together. This clustering results in the formation of groups that, in turn, impact the spreadability and overall workability of SCC by hindering the smooth flow of concrete. Furthermore, the use of PET fibre reduced the thickness of the cement paste, increasing the internal resistance to the flow of surrounding aggregate particles.

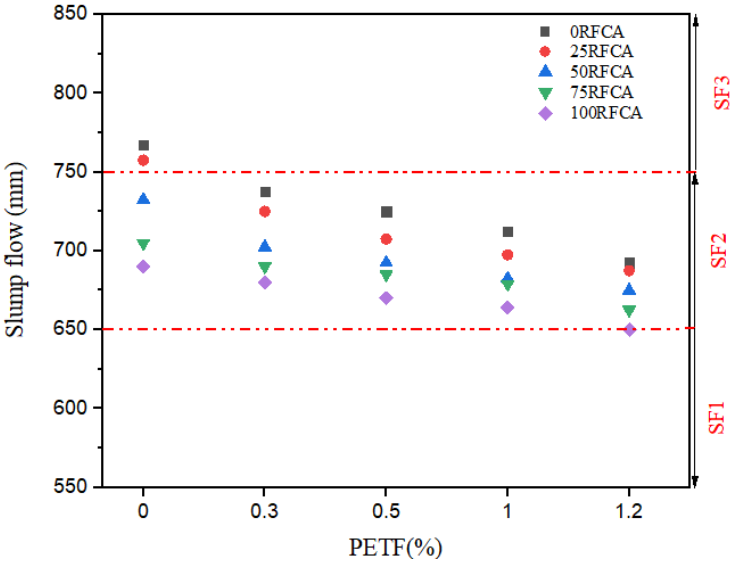

Fig. 4. The effect of PETF and RFCA on the slump flow diameter. *Source:* own study

3.1.2.V-funnel time

The flow time (V-funnel) represents the duration it takes for fresh concrete to flow out of the V-funnel, serving as one of the indicators for investigating concrete viscosity. Fig. 5 depicts the flow timings for all specimens. According to the graph, the flow times for all blends were between 2.55 and 7.89 seconds. The majority of the PETF-RFCA-SCC mixtures met the EFNARC-2005 flow time requirements [21]. However, specimens with 25%, 50%, 75%, and 100% RFCA content were exceptions, with V-funnel timings of 2.98, 3.79, 4.15, and 5.32 seconds, respectively.

Furthermore, as seen in Fig. 5, the flow times for RFCA-SCC mixes increased as the RFCA concentration rose. Notably, the 100% RFCA combination had much higher plastic viscosity, which could result in a reduction of flow capacity. This effect is explained by RFCA's higher powder concentration and increased specific surface area [33].

The effect of PET fibre content on the flow time (V-funnel) of PETF-RFCA-SCC mixes is shown in Fig. 5, where flow time is shown against the PET fibre replacement ratio under varied RFCA replacement ratios. The flow time clearly increased as the PET fibre content increased, as seen in Fig. 5. This is mostly due to the rough surface of PET fibres, which

increased internal friction between the aggregates and friction between the aggregates and fibres. Furthermore, the fibres entangled with the aggregates, restricting aggregate mobility and increasing the viscosity of PETF-RFCA-SCC mixtures. These findings corroborate prior test results reported by Shahidan et al. [34].

Consequently, PETF-RFCA-SCC mixes exhibited increased viscosity and longer flow times. It's worth noting that the flow times (V-funnel) of all specimens remained within the acceptable limits as defined by EFNARC 2005 [21].

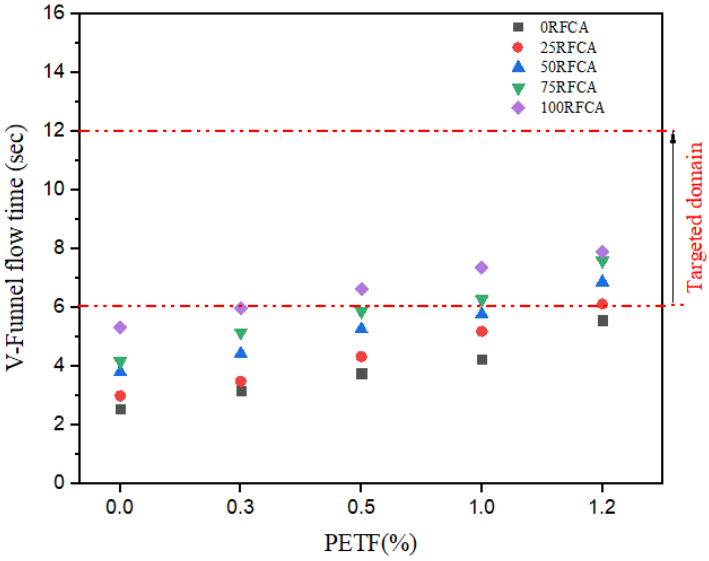

Fig. 5. The effect of PETF and RFCA on the flow time (V-funnel). *Source:* own study

3.1.3.L-box

The H2/H1 ratio values are presented in Fig. 6. A larger H2/H1 value indicates better passing ability. Fig. 6 clearly demonstrates that the H2/H1 levels for all specimens met the EFNARC 2005 standards [21]. This included combinations containing 25%, 50%, 75%, and 100% RFCA, with H2/H1 values of 0.98, 0.96, 0.9, and 0.87, respectively.

Furthermore, as shown in Fig. 6, the H2/H1 value fell as the RFCA content grew, demonstrating that the presence of RFCA had a negative influence on SCC's passing capacity. This can be attributed to the substantial replacement of NFA by RFCA, which led to the presence of adhering old cement mortars and numerous sharp edges on the RFCA particles. These factors resulted in aggregate particles becoming blocked, increasing internal resistance and friction within the concrete. Consequently, this adversely affected the concrete's passing ability.

Fig. 6 depicts the effect of PET fibre content on the passing ability of PETF-RFCA-SCC mixes, where the H2/H1 value is displayed against the PET fibre replacement ratio at various RFCA replacement ratios. Fig. 6 shows that the addition of PET fibre resulted in a drop in the H2/H1 ratio, indicating that PET fibre had a deleterious influence on the passing ability of RFCA-SCC mixtures. The mix with the lowest H2/H1 value was observed in the 100RFCA-1.2PETF mixture. This is due to the larger PET fibre concentration, which increased particle friction and viscosity during concrete flow. As previously discussed in

relation to slump flow time, the increased interlocking and friction caused by higher fibre content most certainly contributed to these less advantageous blocking ratios.

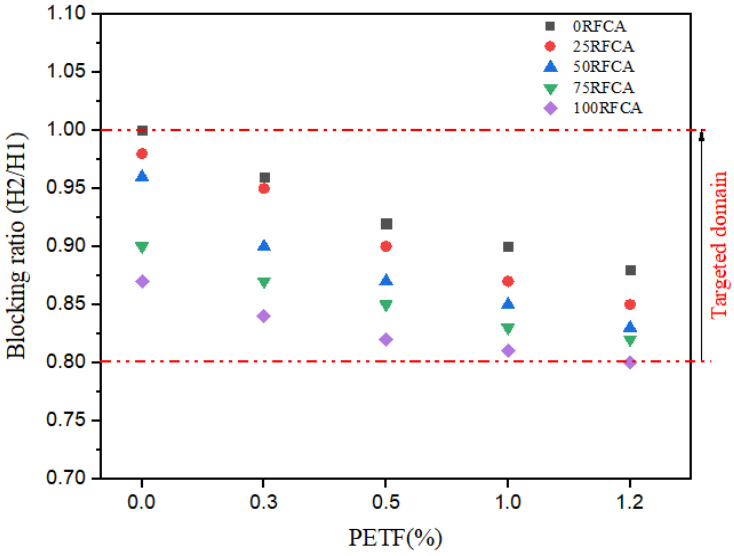

Fig. 6. The effect of PETF and RFCA on the passing ability. *Source:* own study

3.1.4. Sieve stability

Fig. 7 provides a summary of the segregation percentages for all SCC mixes involving various RFCA and PETF. According to the SCC requirements described in EFNARC 2005 [21], the highest permissible segregation rate for SCC blends is 20%, a value commonly recommended to maintain an appropriate level of segregation resistance.

Fig. 7 shows that all PETF-RFCA-SCC mixtures met this condition, indicating that the majority of these mixtures displayed acceptable segregation resistance. Furthermore, Fig. 7 demonstrates that as the RFCA replacement ratio increased, segregation resistance decreased. This decrease can be due to RFCA's increased water absorption capacity.

As shown in Fig. 7, the addition of PET fibre reduced the segregation resistance of PETF-RFCA-SCC mixes. Segregation rates of PETF-RFCA-SCC mixes comprising 100RFCA-1.2PETF were less than 5%, showing poor segregation resistance. PETF-RFCA-SCC mixes containing 0.3% PETF, on the other hand, had good segregation resistance with negligible fibre clumping. This action can be due to the fibres' large surface area, which absorbed and wrapped around the cement paste. As previously discussed, this procedure increased the viscosity and segregation resistance of the concrete mixtures [35].

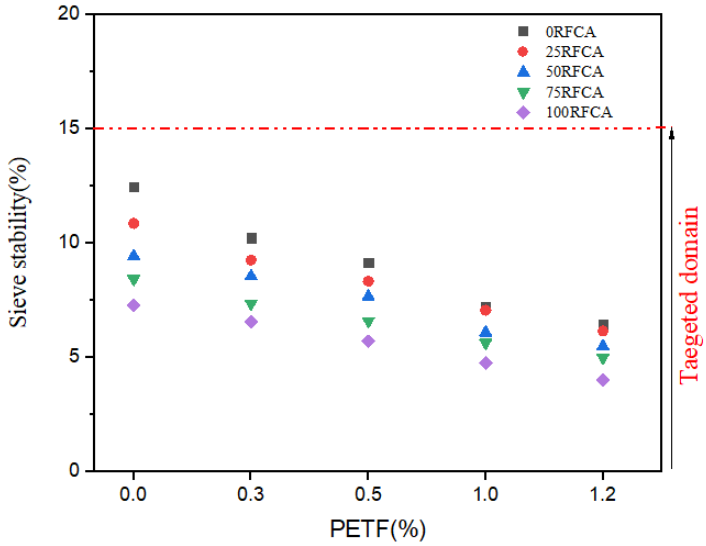

Fig. 7. The effect of PETF and RFCA on the sieve stability test. *Source:* own study

3.2. Hardened concrete properties

3.2.1. Compressive strength

The compressive strength of PETF-RFCA-SCC mixes, with various combinations of PET fibre, is presented in Fig. 8 after 90 days of curing. As depicted in Fig. 8, the compressive strength decreased as the RFCA content increased. Furthermore, it is evident from the figure that 25%, 50%, 75%, and 100% RFCA content led to reductions in compressive strength by 2.38%, 4.93%, 8.59%, and 12.70%, respectively. These findings align with previous research conclusions [33],[35]. The decrease in compressive strength can primarily be attributed to the weaker mechanical properties, higher porosity, and greater water absorption capacity of RFCA when compared to NFA. Furthermore, the creation of microcracks during the RFCA manufacturing process contributed to the decrease in compressive strength.

Fig. 8 depicts the effect of PET fibre content on the compressive strength of RFCA-SCC blends. Fig. 8 shows that the inclusion of PET fibre consistently lowered the compressive strength of PETF-RFCA-SCC mixtures, which is consistent with previous research findings [14],[36],[37]. With the addition of 1% PETF, all PETF-RFCA-SCC mixes showed the greatest increase in compressive strength, outperforming the performance of 0.3%, 0.5%, and 1.2% PETF mixes. For instance, the decrease in cubic compressive strength brought on by the inclusion of 0.3%, 0.5%, 1%, and 1.2% PETF varied from 3.92% to 6.47%, respectively, when compared to reference SCC mixes without RFCA.

Similarly, at 90 days, the cubic compressive strength of 0.3%, 0.5%, 1%, and 1.2% PETF mixes fell by 2.10%, 4.42%, 0.81%, and 3.37%, respectively, when compared to the reference control 100RFCA-SCC mixes without PET fibre. This enhancement can be due to the homogeneous distribution of PET fibre within the recycled concrete's internal structure, which boosted homogeneity and reduced internal voids, hence increasing the compressive strength of PETF-RFCA-SCC mixes when compared to reference RFCA-SCC mixtures.

Finally, when PET fibre volumetric content increased, the compressive strength of RFCA-SCC mixtures decreased. This is due to an increase in PET fibre content, which causes irregular fibre distribution, lowering homogeneity and adhesion between the cement slurry

and fibre surfaces, and resulting in cavities within the concrete. These findings are consistent with the conclusions reached by Ochi et al. [39].

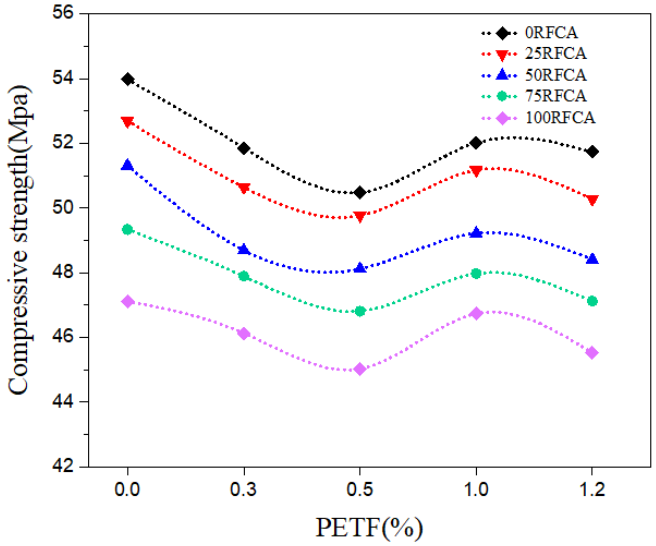

Fig. 8. The effect of PETF and RFCA on the compressive strength. *Source:* own study

Fig. 9 shows a comparison of the experimentally obtained compressive strength values and those calculated using equation (2), producing a correlation coefficient of $R^2 = 0.94$ and a root-mean-square error of 0.65. This indicates the robustness of this correlation.

$$R_{c90}\left(MPa\right) = 53.689 - 0.0595 \cdot R_{RFCA} + 4.467 \cdot R_{PETF}^2 - 6.66 \cdot R_{PETF} \quad (2)$$

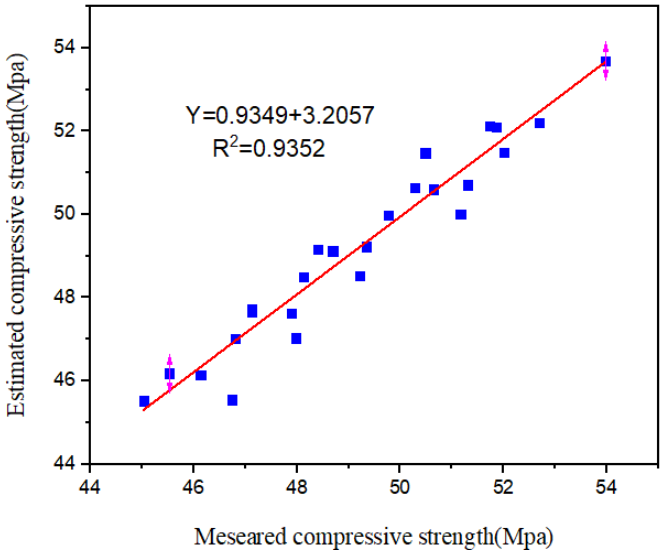

Fig. 9. Comparison of measured and estimated compressive strength of PETF-RFCA-SCC mixes. *Source:* own study

3.2.2. Elastic modulus

Fig. 10 depicts the elastic modulus of RFCA-SCC mixes with various PET fibres. Fig. 10 clearly shows that RFCA-SCC blends have a lower elastic modulus than normal SCC. This reveals that including RFCA in SCC has an effect on the elastic modulus of RFCA-SCC mixtures, with a drop ranging from 5.01% to 19.30%.

It is generally acknowledged that the substitution of RFCA has a significant impact on the elastic modulus of concrete. The decrease in this modulus when using RFCA can be attributed to factors such as the interfacial transition zone and the presence of a porous microstructure, both of which are associated with the adhered cement paste on the surface of RFCA. Many studies in the literature have reported on the impact of RFCA replacement on the elastic modulus of concrete, highlighting its significant effect [39],[40].

Furthermore, earlier research has consistently shown that the inclusion of PET fibres increases the elastic modulus of SCC [14]. Fig. 10 indicates, however, that the addition of PET fibre can mitigate the negative influence of RFCA and increase the elastic modulus of RFCA-SCC mixes. Compared to the 100RFCA-SCC combination, mixes containing 0.3%, 0.5%, 1%, and 1.2% PETF increased the modulus by 11.40%, 13.29%, 17.21%, and 24.87%, respectively.

This improvement can be attributed to the increased bond strength between the PET fibre and other components of the concrete mixture, resulting from the lack of convergence and the spacing of the fibres [14].

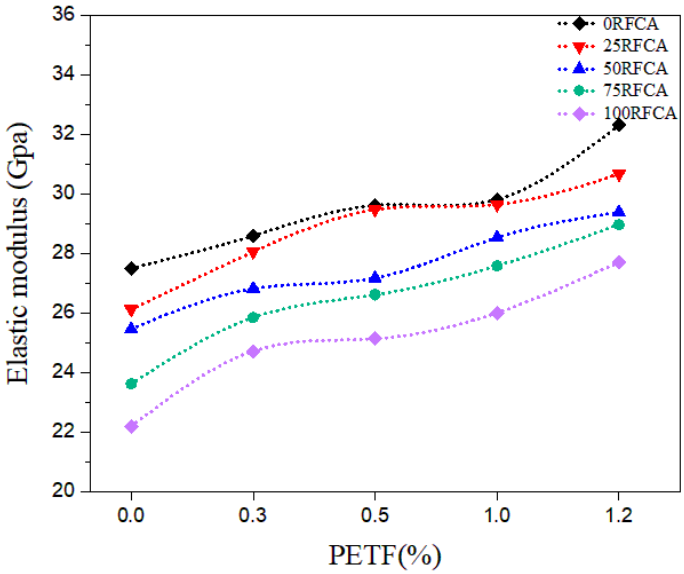

Fig. 10. The effect of PETF and RFCA on the elastic modulus. *Source:* own study

To express the change in the elastic modulus of SCC as a function of both PET fibre and RFCA content, multiple relationships were investigated to find the one with the highest correlation coefficient. The outcome yielded the following relationship for estimating the elastic modulus at 90 days of curing:

$$E_{90}\left(GPa\right) = 27.455 - 0.045 \cdot R_{RFCA} - 1.564 \cdot R_{PETF}^2 + 5.369 \cdot R_{PETF} \tag{3}$$

Here, R_{RFCA} represents the rate of RFCA substitution for NFA, and R_{PETF} represents the rate of PETF. As seen in Fig. 11, this relationship gives a good match with a correlation coefficient of 0.95 and a root mean square error of 0.62%. This equation effectively captures the combined effects of RFCA and PETF, where RFCA results in a linear decrease in elastic modulus, while PETF contributes to an increase in this modulus.

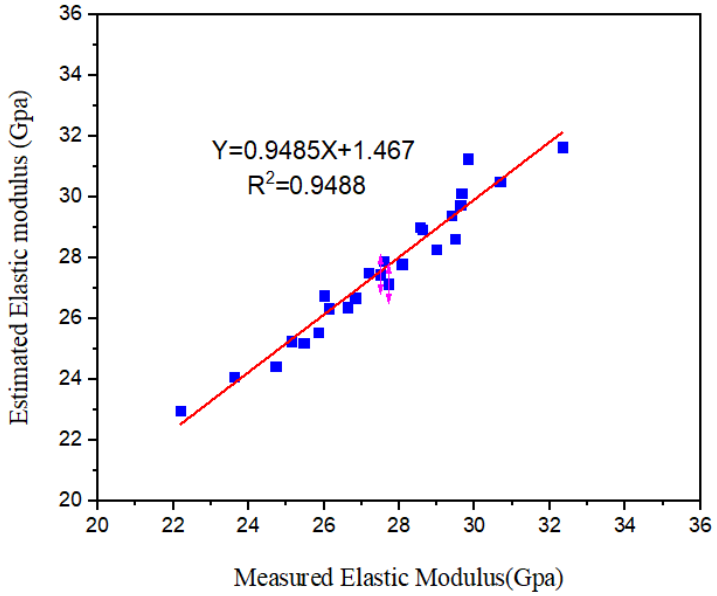

Fig. 11. Comparison of measured and estimated Elastic modulus of PETF-RFCA-SCC mixes. *Source:* own study

3.2.3. Flexural strength

Fig. 12 illustrates the flexural strength of every RFCA-SCC mixture with a range of PET fibre contents. This figure clearly shows that the flexural strength of all RFCA specimens was lower than that of the control mix. For instance, the specimen with a replacement ratio of 25% exhibited a reduction of 2.5% compared to the reference concrete, while the specimen with a replacement of 100% saw a reduction of 25.3% compared to the reference concrete.

This decrease in flexural strength can be attributed to the higher water absorption capacity of RFCA, which reduces the interfacial bonding capacity between recycled aggregate and cement paste [42].

Notably, there was an enhancement in flexural strength attributed to the addition of PET fibre. Furthermore, flexural strength increased as the PETF content increased, ranging from 3.43% to 19.2%. Furthermore, the inclusion of PETF had a greater positive influence on enhancing flexural strength than compressive strength. In other words, the increase in flexural strength was greater than the rise in compressive strength. This is mostly due to the localized limitations established by PETF reinforcement, which effectively regulate the development of fractures prior to the emergence of obvious macro cracks. These fibres also withstand the tension pressures created in the beam specimens, increasing the flexural strength of the concrete [43].

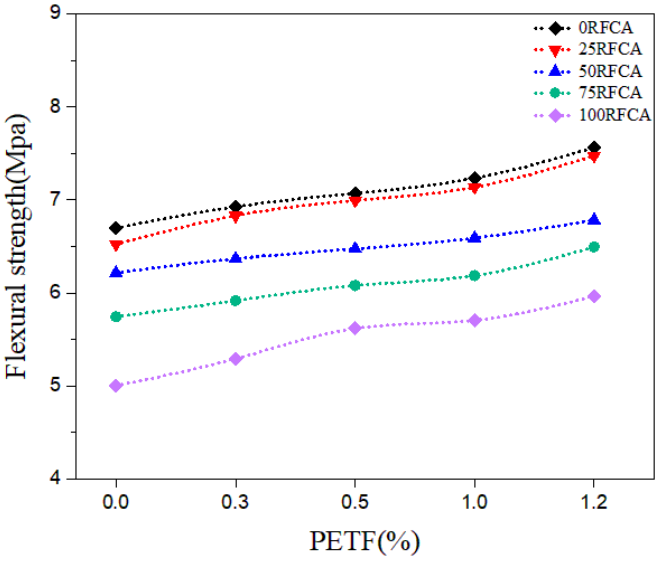

Fig. 12. The effect of PETF and RFCA on the flexural strength. *Source:* own study

Several mathematical equations were investigated to depict the flexural strength of SCC in relation to the replacement rates of RFCA and PET fibre. The most compelling conclusion is a polynomial relationship between the two substitution rates, with a strong correlation coefficient of $R^2 = 0.95$. Fig. 13 compares the measured and estimated flexural strength of several SCC mixtures. This relationship can be expressed as follows:

$$R_{T90}\left(MPa\right) = 6.885 - 0.016 \cdot R_{RFCA} + 0.607 \cdot R_{PETF} \tag{4}$$

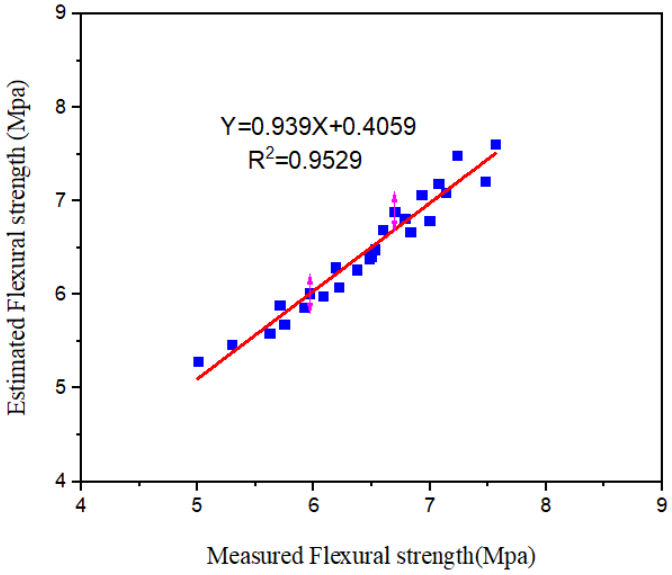

Fig. 13. Comparison of measured and estimated flexural strength of PETF-RFCA-SCC mixes. *Source:* own study

3.2.4. Water absorption by immersion

The results of the water absorption by immersion test for all PETF-RFCA-SCC mixtures are presented in Fig. 14. Water absorption tests are conducted to assess the durability of concrete, as they indicate the sample's ability to absorb water that may contain harmful agents. This test also provides a general approximation of pore connectivity within the sample's microstructure. As expected in this test, water absorption increased with the presence of RFCA and PETF. Due to the surface of the fibre and the substitution of NFA by RFCA, water absorption increased by 10.70%, 37.42%, 58.98%, and 92.66% accordingly at substitution levels of 25%, 50%, 75%, and 100% of RFCA. These water absorption values are associated with the nature of RFCA, characterised by a higher absorption coefficient and high porosity. Another aspect that may have influenced this result was the reduced unitary mass of this granulometric composition, indicating the presence of larger voids [31].

According to the results in Fig. 14, it is also observed that the water absorption capacity increases with the addition of PET fibre. Water absorption values vary between 3.01% and 4.28% in the series of SCC with 0.3%, 0.5%, 1%, and 1.2% of PET fibre. This is because the volume of permeable voids inside the concrete is influenced by the connectivity of pores within the concrete. These results demonstrate that the addition of fibre has enhanced the connectivity between pores and microchannels, resulting in greater absorption [44].

According to Fig. 14, the control mix has the lowest absorption coefficient, while the absorption coefficient of the other mixtures is higher, and it increases as the content of RFCA and PETF increases. Based on the results obtained, a significant increase in water absorption is noted in the mix 100RFCA-SCC. This increase was approximately 19.18%, 21.49%, 26.16%, and 29.86% for the mixtures with 0.3%, 0.5%, 1% and 1.2% of PET fibre respectively.

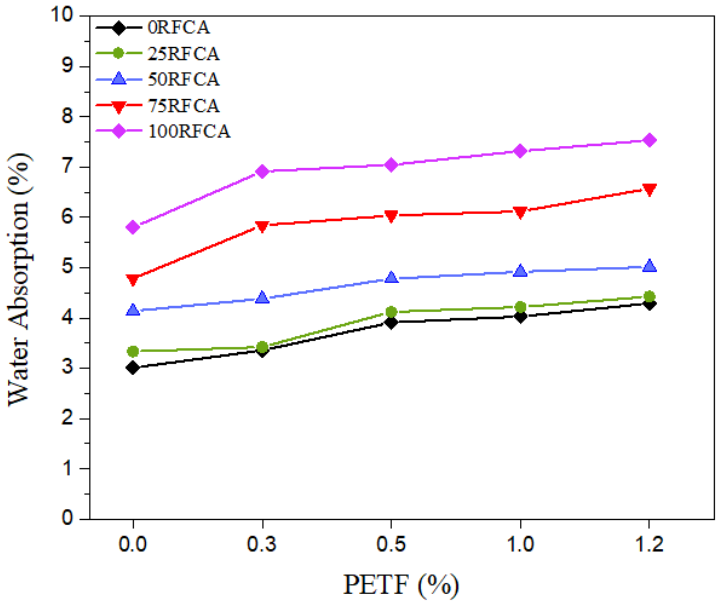

Fig. 14. The effect of PETF and RFCA on the water absorption. *Source:* own study

It is advisable to represent the changes in water absorption for SCC in relation to the levels of RFCA and PETF. To achieve this, various relationships were examined to identify the one that exhibited the strongest correlation, indicated by the highest correlation coefficient. The outcome provides the water absorption values after a 90-day treatment, as expressed by the following correlation:

$$R_b(\%) = 2.865 - 0.00025 \cdot R_{RFCA}^2 + 0.008 \cdot R_{RFCA} - 0.943 \cdot R_{PETF}^2 + 2.174 \cdot R_{PETF} \quad (5)$$

In this context, R_{RFCA} represents the proportion of RFCA that replaces NFA, while R_{PETF} signifies the proportion of PETF content. This correlation demonstrates a robust fit, with a correlation coefficient of 0.99 and a root mean square error of only 0.2%, as depicted in Fig. 15. This relationship reflects how these two materials collectively result in a linear rise in water absorption.

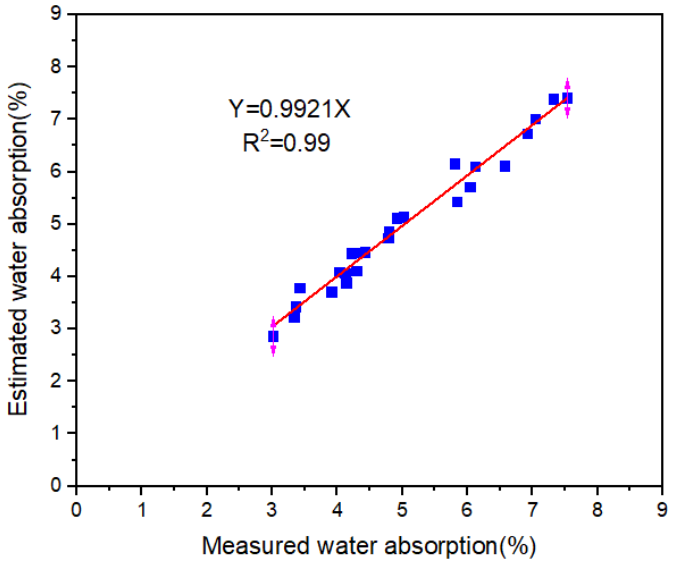

Fig. 15. Comparison of measured and estimated water absorption of PETF-RFCA-SCC mixes. *Source:* own study

3.2.5. Capillary water absorption.

The water absorption by capillarity test of RFCA-SCC mixes with various PET fibres at different times is presented in Fig. 16. An increased amount of RFCA in the SCC mix led to an increase in capillary water absorption. This increase can be attributed to the high-water absorption capacity of RFCA, and also due to the bulk density presented by the RFCA. The cement paste may have been insufficient to cover the existing spaces between the aggregates, resulting in a larger void ratio and increased absorption [31]. The capillarity absorption values for different substitutions of RFCA varied from 1.59% to 3.52% at 7 days, with 100% RFCA substitution resulting in the highest water absorption value. However, it can be observed from Fig. 16 that PETF-RFCA-SCC mixes exhibited increased capillarity absorption compared to the control mix (SCC). This suggests that the addition of PET fibres in the RFCA-SCC mixes increased water absorption. This increase may be attributed to the irregular distribution of fibres when increasing the volumetric ratios of fibres, leading to the entrapment of air voids beneath the lamellar body [45].

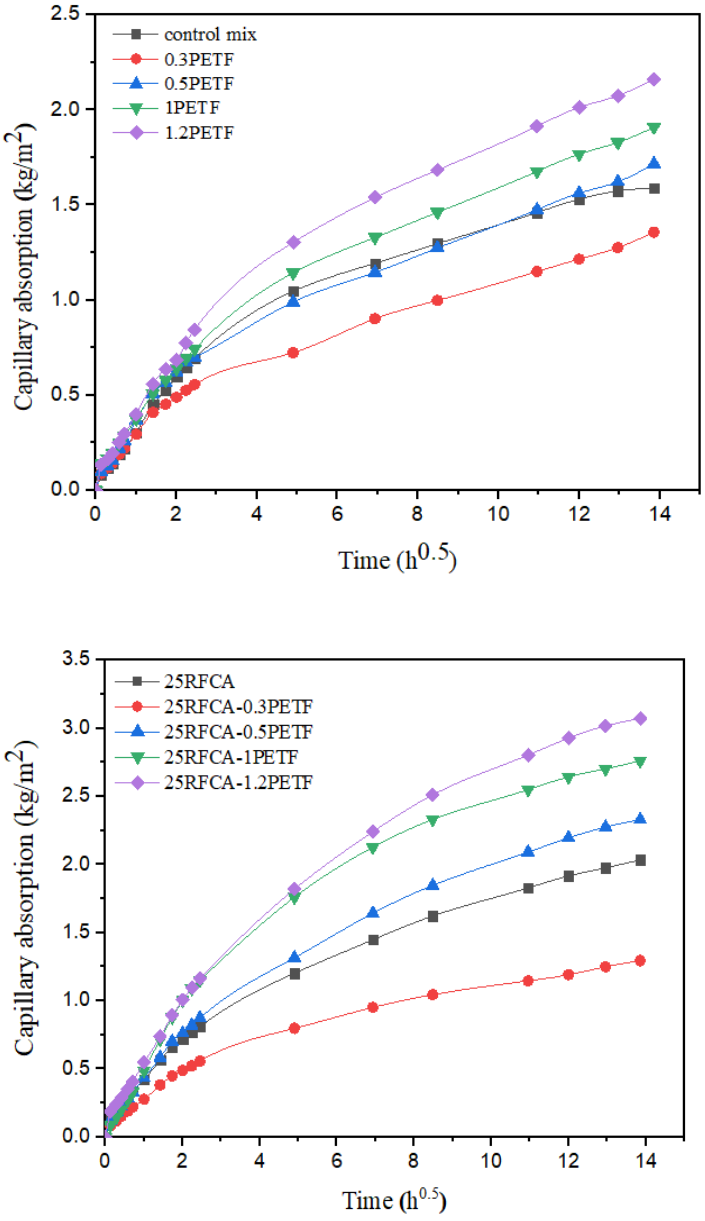

Fig. 16. The effect of PETF and RFCA on the capillary water absorption. *Source:* own study

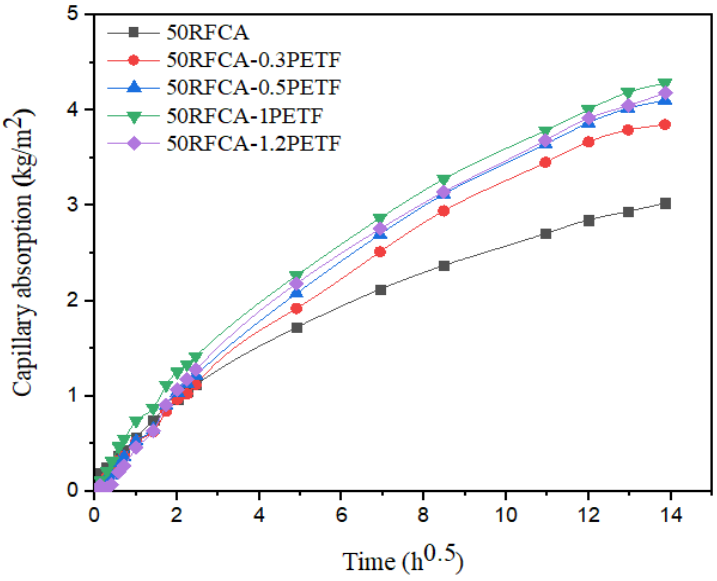

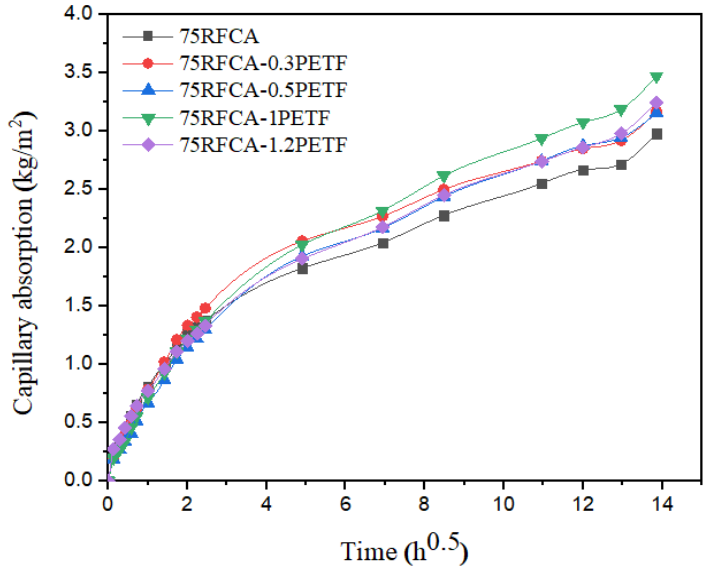

Fig. 16 (cont.). The effect of PETF and RFCA on the capillary water absorption. *Source:* own study

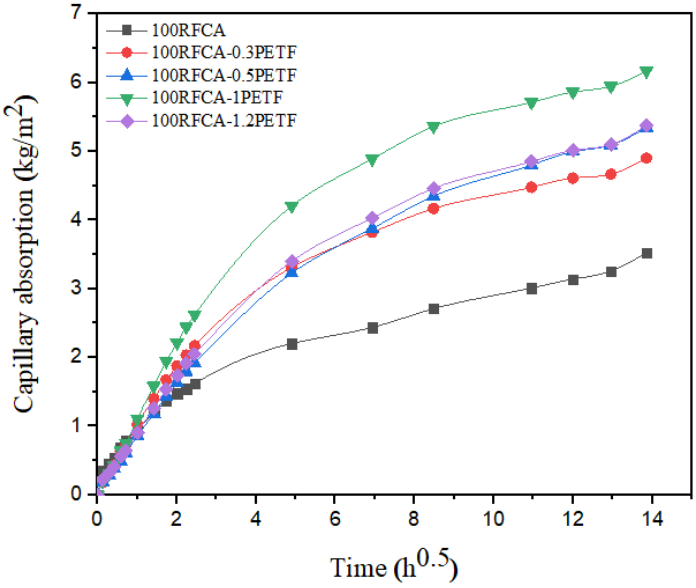

Fig. 16 (cont.). The effect of PETF and RFCA on the capillary water absorption. *Source:* own study

3.2.6. Microstructure analysis

Fig. 17 displays images generated during Scanning Electron Microscopy (SEM) analysis, showcasing the interfacial transition zone (ITZ) between cement pastes and aggregates in both the control mix and the RFCA-SCC mixes with varying amounts of RFCA substitution. The microstructure of the ITZ, as depicted in Fig. 17, predominantly consists of aggregate material, fractures, unhydrated particle fragments, cement mortar, and pores. In comparison to the ITZ of the control mix (Fig. 17a), the ITZ of RFCA-SCC exhibits significantly larger and wider microcracks and pores. This occurrence is mainly due to the presence of aged mortars adhering to the RFCA and the formation of microcracks during RFCA production. Consequently, RFCA displays a higher capacity for water absorption. As a result, a considerable amount of internal water accumulates, forming a porous $Ca(OH)_2$-rich layer between the RFCA and cement pastes at the ITZ, increasing the presence of micropores and cracks within the ITZ and reducing its strength [19]. Furthermore, the hardening shrinkage of the cement paste causes internal tension within the ITZ, resulting in the separation of aggregates and cement paste. This gap weakens the bond between the aggregate and cement paste. Additionally, Fig. 17c illustrates that the mixes with 100% RFCA exhibit wider cracks and more pores, indicating that an increased RFCA content has an unfavourable impact on the quality of the ITZ. The microstructures of the interfacial transition zone (ITZ) between cement paste and PET fibre were examined at various magnifications, as depicted in Fig. 17. The figure clearly illustrates PET fibres embedded in the cement mix and surrounded by hydration products. This not only prevents the separation of PETF-RFCA-SCC mixes and the formation of settlement fractures but also plays a synergistic role in bridging cracks, thereby enhancing the strength and toughness of RFCA-SCC mixes [19].

Fig. 17(b) shows minor microcracks and pores in the ITZ between cement paste and PET fibres. These can be attributed to the surface of PET fibres. The inclusion of fibres in

this sample enhances the strength of RFCA-SCC, preventing it from easily breaking into two pieces under flexural or tensile splitting forces. This improvement can be attributed to the friction created between the fibre surfaces and the surrounding cement paste.

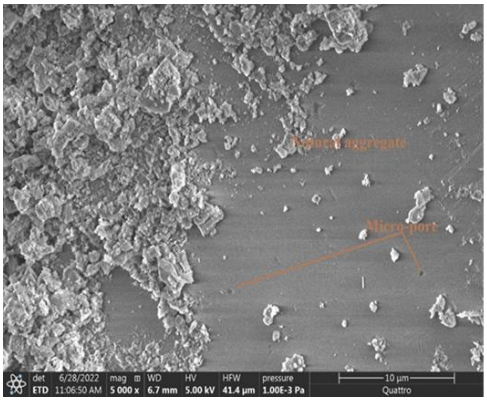

a) Contro mix

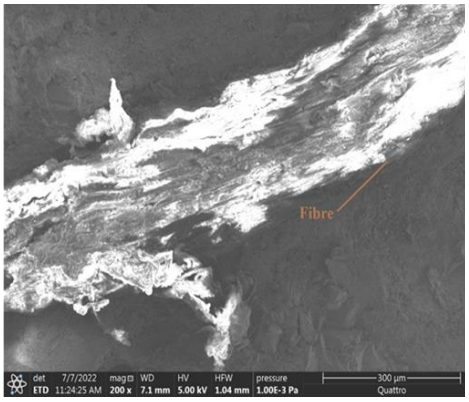

b) 0RFCA-1.2PETF

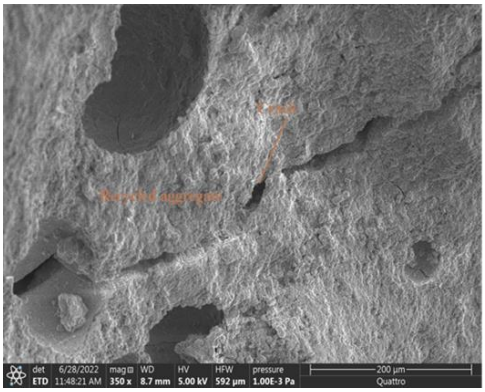

c) 100RFCA -1.2PETF

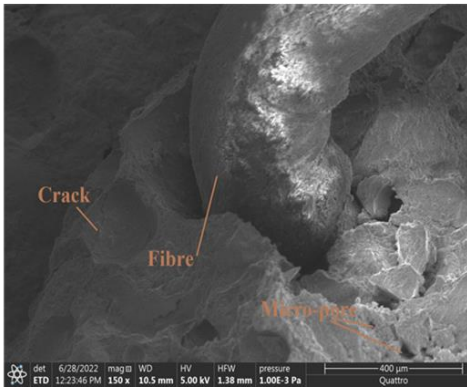

d) 100 RFCA-1.2PETF

Fig. 17. SEM images of typical specimens. *Source:* own study

4. Conclusions

The purpose of this paper is to elucidate the findings of an experimental investigation aimed at assessing the influence of PETF and RFCA on the behaviour of self-compacting concrete. The current study yields the following conclusions:

- The workability of SCC is negatively affected by the presence of PETF and RFCA. The higher the percentage of PETF and RFCA, the lower the concrete's flowability. This decline is primarily attributed to RFCA's high water absorption and PETF's specific surface.
- Increasing the proportion of fibers has a greater impact on concrete's workability, leading to an increase in viscosity that can result in segregation and potential blockages within the mixture.

- The addition of a small amount of SP can significantly enhance the flowability of RSCC.
- The compressive strength of SCC decreases as the percentage of PETF and RFCA increases. It is recommended not to exceed 25-50% of RFCA and 1% of PETF for optimal results.
- The incorporation of PETF significantly improves the flexural strength and modulus of elasticity of concrete containing various RFCA.
- A reduction in flexural strength at 90 days is observed when 100% of RCFA is substituted, but adding 1.2% of PETF increases flexural strength by 19%.
- The modulus of elasticity behaves similarly to compressive strength, with a 19% decrease noted for 100% of RFCA. However, the addition of 1.2% of PETF increases the modulus of elasticity of RSCC by 25%.
- The inclusion of RFCA significantly increases water absorption when SCC mixes are immersed, with the highest increase (92%) occurring at 100% RFCA usage. Additionally, the simultaneous introduction of PETF and RFCA has a marginal influence on the SCC mix, resulting in a water absorption increase ranging from 2.61% to 37.35%.
- The incorporation of RFCA and PET fibres in SCC leads to higher capillary water absorption compared to RFCA-SCC mixes without PET fibres. The particle size distribution of RFCA, along with their mineralogical composition, significantly influences SCC properties.
- Various characteristics of self-compacting concrete can be described using straightforward equations that depend on RFCA and PET fibres concentrations. Strong correlation coefficients and minimal root-mean-square errors support the suitability of these equations, emphasizing the impact of each ingredient on the production of self-compacting concrete.

As a result, when utilizing recycled aggregates, a specific approach is essential to ensure that the concrete employed possesses the necessary properties. One potential solution to enhance the properties of Recycled Concrete with Sustainable Concrete (RSCC) involves the incorporation of PETFs. This addition has the potential to reinforce RSCC and subsequently improve its overall characteristics. However, it is crucial to emphasize the need for safety measures and precautions, particularly in terms of preventing reinforcement blockage or concrete segregation, when working with fresh concrete. Additionally, further research is required to investigate the source, nature, and type of contamination in the recycled aggregates (RAs) and their potential impact on the composite, as this could pose a potential hazard.

References

[1] H. Lv, Y. Li, H. Bin Yan, D. Wu, G. Shi, and Q. Xu, “Examining construction waste management policies in mainland China for potential performance improvements,” *Clean Technol. Environ. Policy*, vol. 23, no. 2, pp. 445–462, 2021. https://doi.org/10.1007/s10098-020-01984-y

[2] L. W. Zhang, A. O. Sojobi, V. K. R. Kodur, and K. M. Liew, “Effective utilization and recycling of mixed recycled aggregates for a greener environment,” *J. Clean. Prod.*, 2019. https://doi.org/10.1016/j.jclepro.2019.07.075

[3] M. U. Hossain, C. S. Poon, I. M. C. Lo, and J. C. P. Cheng, “Comparative environmental evaluation of aggregate production from recycled waste materials and virgin sources by LCA,” *Resour. Conserv. Recycl.*, vol. 109, pp. 67–77, 2016. https://doi.org/10.1016/j.resconrec.2016.02.009

[4] L. W. Zhang, A. O. Sojobi, and K. M. Liew, "Sustainable CFRP-reinforced recycled concrete for cleaner eco-friendly construction," *J. Clean. Prod.*, vol. 233, pp. 56–75, 2019. https://doi.org/10.1016/j.jclepro.2019.06.025

[5] A. Ait Mohamed Amer, K. Ezziane, and M. H. Adjoudj, "Evaluation of coarse recycled concrete aggregates effect on the properties of fresh and hardened concrete," *Asian J. Civ. Eng.*, vol. 22, no. 6, pp. 1173–1184, 2021. https://doi.org/10.1007/s42107-021-00373-0

[6] Y. Toumi, S. Mezhoud, O. Boukendakdji, and H. Moussa, "Impact of recycled aggregate brick on the physical-mechanical and environmental characteristics of cement treated bases Impact of recycled aggregate brick on the physical-mechanical and environmental characteristics of cement treated bases," no. September, 2023. https://doi.org/10.35784/bud-arch.3645

[7] K. Kapoor, S. P. Singh, B. Singh, and P. Singh, "Effect of recycled aggregates on fresh and hardened properties of self compacting concrete," *Mater. Today Proc.*, vol. 32, no. xxxx, pp. 600–607, 2020. https://doi.org/10.1016/j.matpr.2020.02.753

[8] E. Güneyisi, M. Gesoglu, Z. Algin, and H. Yazici, "Rheological and fresh properties of self-compacting concretes containing coarse and fine recycled concrete aggregates," *Constr. Build. Mater.*, vol. 113, pp. 622–630, 2016. https://doi.org/10.1016/j.conbuildmat.2016.03.073

[9] M. U. Usmani and A. S. M. A. Awal, "Physical, mechanical and durable characteristics of concrete incorporating polyethylene terephthalate fiber from bottle waste," *J. Crit. Rev.*, vol. 7, no. 5, pp. 908–916, 2020. https://doi.org/10.31838/jcr.07.05.187

[10] L. Evangelista and J. de Brito, "Durability performance of concrete made with fine recycled concrete aggregates," *Cem. Concr. Compos.*, vol. 32, no. 1, pp. 9–14, 2010. https://doi.org/10.1016/j.cemconcomp.2009.09.005

[11] D. Nieto, E. Dapena, P. Alaejos, J. Olmedo, and D. Pérez, "Properties of Self-Compacting Concrete Prepared with Coarse Recycled Concrete Aggregates and Different Water:Cement Ratios," *J. Mater. Civ. Eng.*, vol. 31, no. 2, p. 04018376, 2019. https://doi.org/10.1061/(asce)mt.1943-5533.0002566

[12] M. Pająk, "Research on the recycled and hybrid fibre reinforced self-compacting concrete under flexure," *Bud. i Archit.*, vol. 19, no. 3, pp. 116–126, 2020. https://doi.org/10.35784/bud-arch.2150

[13] J. A. Carneiro, P. R. L. Lima, M. B. Leite, and R. D. Toledo Filho, "Compressive stress-strain behavior of steel fiber reinforced-recycled aggregate concrete," *Cem. Concr. Compos.*, vol. 46, pp. 65–72, 2014. https://doi.org/10.1016/j.cemconcomp.2013.11.006

[14] A. H. Allawi, A. I. Al-hadithi, and A. S. Mohmoud, "Iraqi Journal of Civil Engineering Effects of Waste Plastic PET Fibers on The Fresh and Hardened of Normal Concrete," 2021.

[15] I. Zemir, F. Debieb, S. Kenai, Y. Ouldkhaoua, and I. Irki, "Strengthening of ordinary vibrated concrete using steel fibers self-compacting concrete," *J. Adhes. Sci. Technol.*, vol. 34, no. 14, pp. 1556–1571, 2020. https://doi.org/10.1080/01694243.2020.1712769

[16] A. I. Al-hadithi, A. Tareq, and W. Khairi, "Mechanical properties and impact behavior of PET fi ber reinforced self- compacting concrete (SCC)," *Compos. Struct.*, vol. 224, no. May, p. 111021, 2019. https://doi.org/10.1016/j.compstruct.2019.111021

[17] N. K. Bui, T. Satomi, and H. Takahashi, "Recycling woven plastic sack waste and PET bottle waste as fiber in recycled aggregate concrete: An experimental study," *Waste Manag.*, vol. 78, pp. 79–93, 2018. https://doi.org/10.1016/j.wasman.2018.05.035

[18] M. Hajmohammadian Baghba, S. A. H. Hashemi, K. Kalbasi Anaraki, and E. S. Hashemi, "Influence of polypropylene-fiber on the mechanical properties of self-compacting-concrete with recycled aggregates," *Mag. Civ. Eng.*, vol. 99, no. 7, 2020. https://doi.org/10.18720/MCE.99.5

[19] C. Dong *et al.*, "Fresh and hardened properties of recycled plastic fiber reinforced self-compacting concrete made with recycled concrete aggregate and fly ash, slag, silica fume," *J. Build. Eng.*, vol. 62, no. September, p. 105384, 2022. https://doi.org/10.1016/j.jobe.2022.105384

[20] A. Toghroli, P. Mehrabi, M. Shariati, N. T. Trung, S. Jahandari, and H. Rasekh, "Evaluating the use of recycled concrete aggregate and pozzolanic additives in fiber-reinforced pervious concrete

with industrial and recycled fibers," *Constr. Build. Mater.*, vol. 252, 2020. https://doi.org/10.1016/j.conbuildmat.2020.118997

[21] P. and U. EFNARC The European Guidelines for Self-Compacting Concrete: Specification, "The European Guidelines for Self-Compacting Concrete: Specification, Production and Use," *Eur. Guidel. Self Compact. Concr.*, no. May, p. 68, 2005.

[22] BS EN 12350-8:2010, "BSI Standards Publication Testing fresh concrete," *Br. Stand.*, no. April, p. 18, 2010.

[23] N. F. EN, "12350–10, Novembre 2010," *Partie Bét. autoplaçant–essai à la boite en L*.

[24] 2010 BS EN12350-11:, "BSI Standards Publication Testing fresh concrete Part 11: Self-compacting concrete -- sieve Segregation test," *BSI Stand. Publ.*, 2010.

[25] B. S. I. BSI, "12390-3 Testing hardened concrete Compressive strength of test specimens," *Aberdeen's Concr. Constr.*, vol. 38, no. 10, 1993.

[26] ASTM C469/C469M, "Standard Test Method for Static Modulus of Elasticity and Poisson's Ratio of Concrete in Compression," *ASTM Stand. B.*, pp. 1–5, 2014. https://doi.org/10.1520/C0469

[27] British Standards Institute, "BS EN 12390-5:2009 Testing hardened concrete — Part 5: Flexural strength of test specimens," *BSI Stand. Publ.*, no. August, pp. 1–22, 2009.

[28] "BS 1881-122_2011 Testing concrete."

[29] "ASTM C1585_Measurement of Rate of Absorption of Water by HydraulicCement Concretes."

[30] D. Carro-López, B. González-Fonteboa, J. De Brito, F. Martínez-Abella, I. González-Taboada, and P. Silva, "Study of the rheology of self-compacting concrete with fine recycled concrete aggregates," *Constr. Build. Mater.*, vol. 96, pp. 491–501, 2015. https://doi.org/10.1016/j.conbuildmat.2015.08.091

[31] P. Kruger, P. Serbai, A. S. A. Chinelatto, and E. Pereira, "Influence of particle size distribution of conventional fine aggregate and construction demolition waste aggregate in Portland cement mortar," *Ceramica*, vol. 67, no. 383, pp. 269–276, 2021. https://doi.org/10.1590/0366-69132021673833035

[32] A. I. Al-Hadithi and N. N. Hilal, "The possibility of enhancing some properties of self-compacting concrete by adding waste plastic fibers," *J. Build. Eng.*, vol. 8, pp. 20–28, 2016. https://doi.org/10.1016/j.jobe.2016.06.011

[33] N. Bahrami, M. Zohrabi, S. A. Mahmoudy, and M. Akbari, "Optimum recycled concrete aggregate and micro-silica content in self-compacting concrete: Rheological, mechanical and microstructural properties," *J. Build. Eng.*, vol. 31, no. February, p. 101361, 2020. https://doi.org/10.1016/j.jobe.2020.101361

[34] S. Shahidan, N. A. Ranle, S. S. M. Zuki, F. S. Khalid, A. R. M. Ridzuan, and F. M. Nazri, "Concrete incorporated with optimum percentages of recycled polyethylene terephthalate (PET) bottle fiber," *Int. J. Integr. Eng.*, vol. 10, no. 1, pp. 1–8, 2018. https://doi.org/10.30880/ijie.2018.10.01.001

[35] M. Oghabi and M. Khoshvatan, "The Laboratory Experiment of the Effect of Quantity and Length of Plastic Fiber on Compressive Strength and Tensile Resistance of Self-Compacting Concrete," *KSCE J. Civ. Eng.*, vol. 24, no. 8, pp. 2477–2484, 2020. https://doi.org/10.1007/s12205-020-1578-9.

[36] A. G. Khoshkenari, P. Shafigh, M. Moghimi, and H. Bin Mahmud, "The role of 0-2mm fine recycled concrete aggregate on the compressive and splitting tensile strengths of recycled concrete aggregate concrete," *Mater. Des.*, vol. 64, pp. 345–354, 2014. https://doi.org/10.1016/j.matdes.2014.07.048

[37] O. Gencel, W. Brostow, T. Datashvili, and M. Thedford, "Workability and mechanical performance of steel fiber-reinforced self-compacting concrete with fly ash," *Compos. Interfaces*, vol. 18, no. 2, pp. 169–184, 2011. https://doi.org/10.1163/092764411X567567

[38] M. Ahmadi, S. Farzin, A. Hassani, and M. Motamedi, "Mechanical properties of the concrete containing recycled fibers and aggregates," *Constr. Build. Mater.*, vol. 144, pp. 392–398, 2017. https://doi.org/10.1016/j.conbuildmat.2017.03.215

[39] T. Ochi, S. Okubo, and K. Fukui, "Development of recycled PET fiber and its application as concrete-reinforcing fiber," *Cem. Concr. Compos.*, vol. 29, no. 6, pp. 448–455, 2007. https://doi.org/10.1016/j.cemconcomp.2007.02.002

[40] M. Behera, A. K. Minocha, and S. K. Bhattacharyya, "Flow behavior, microstructure, strength and shrinkage properties of self-compacting concrete incorporating recycled fine aggregate," *Constr. Build. Mater.*, vol. 228, p. 116819, 2019, https://www.doi.org/10.1016/j.conbuildmat.2019.116819

[41] D. Pedro, J. de Brito, and L. Evangelista, "Structural concrete with simultaneous incorporation of fine and coarse recycled concrete aggregates: Mechanical, durability and long-term properties," *Constr. Build. Mater.*, vol. 154, pp. 294–309, 2017. https://doi.org/10.1016/j.conbuildmat.2017.07.215

[42] E. Ghorbel and G. Wardeh, "Influence of recycled coarse aggregates incorporation on the fracture properties of concrete," *Constr. Build. Mater.*, vol. 154, pp. 51–60, 2017. https://doi.org/10.1016/j.conbuildmat.2017.07.183

[43] J. Nam *et al.*, "Effectiveness of fiber reinforcement on the mechanical properties and shrinkage cracking of recycled fine aggregate concrete," *Materials (Basel).*, vol. 9, no. 3, 2016. https://doi.org/10.3390/ma9030131

[44] M. Koushkbaghi, M. J. Kazemi, H. Mosavi, and E. Mohseni, "Acid resistance and durability properties of steel fiber-reinforced concrete incorporating rice husk ash and recycled aggregate," *Constr. Build. Mater.*, vol. 202, pp. 266–275, 2019. https://doi.org/10.1016/j.conbuildmat.2018.12.224

[45] A. I. Al-hadithi and W. K. M. Frhaan, "The Effects of Adding Waste Plastic Fibers (WPFs) on Some Properties of Self Compacting Concrete using Iraqi local Materials," *Iraqi J. Civ. Eng.*, vol. 11, no. 1, pp. 1–20, 2017.